Rotational Cars - A Comparison of Different Techniques With Emphasis On Accuracy In Temperature Determination

Aldén, Marcus; Bengtsson, Per-Erik; Edner, H; Kröll, Stefan; Nilsson, D

Published in:
Optical Society of America. Journal B: Optical Physics

DOI:
10.1364/AO.28.003206

1989

Rotational CARS: a comparison of different techniques with emphasis on accuracy in temperature determination

Marcus Aldén, Per-Erik Bengtsson, Hans Edner, Stefan Kröll, and David Nilsson

Different rotational CARS techniques have been evaluated in terms of single-shot temperature accuracy and signal intensity in room temperature nitrogen and in flames. The different techniques include both dual broadband techniques, using one or two broadband dye lasers, and conventional rotational CARS with different dye lasers. These techniques are also compared with vibrational CARS concerning temperature accuracy and with theoretical predictions. The results indicate that the dual broadband techniques are to be preferred over conventional rotational CARS and also over vibrational CARS at room temperature. At flame temperatures the vibrational CARS technique seems to be the technique yielding highest temperature accuracy. The experimental results are also generally in good agreement with the calculated values.

I. Introduction

During the last decade global awareness of our limited natural resources and fragile environmental situation has strongly encouraged basic research directed toward a deeper understanding of different combustion processes. In this respect, areas such as chemical kinetics, turbulent modeling, and different diagnostic techniques are of vital importance. The latter field has experienced a renaissance with the introduction of various techniques based on the application of lasers. The first laser was constructed in the early sixties, and during the last fifteen years lasers have begun to be used in real combustion applications (see, e.g., Refs. 1 and 2).

The technique which is most commonly thought to have the largest potential for flame diagnostics, at least in a real-world combustion environment, is coherent anti-Stokes Raman scattering (CARS). Since the first application of CARS to a combustion system, by Taran and co-workers in the early seventies,[3] CARS has been developed to yield measurements with high spatial and temporal resolution with the introduction of the BOXCARS[4] and broadband CARS[5] techniques. Probing of vibrational–rotational state populations using CARS, normally referred to as vibrational CARS, has been used in numerous applications including several real-world situations (see, e.g., Refs. 6–9).

An alternative to vibrational CARS is to probe pure rotational transitions, i.e., rotational CARS, which also seems promising in many respects. In general, the linewidths are narrower and the cross sections larger than those for vibrational CARS. This favors the rotational CARS signal intensity. Since the rotational constant for a molecule (except for H_2) is $<20\ cm^{-1}$, it is also possible to measure several species simultaneously using only one dye laser. Another advantage with rotational CARS is that the individual lines are, in general, well separated ($\sim 8\ cm^{-1}$ for N_2) which means that a computer code describing the spectral shape does not require inclusion of effects such as collisional narrowing and also that the detection system instrument function can be unambiguously determined from the spectrum. However, in comparison with vibrational CARS, there have been relatively few reports on pure rotational CARS and very few applications of this technique to flame diagnostics. The main reasons for this have been problems with suppression of the much stronger laser beams (in comparison with the CARS beam), poor dye efficiency when using a Nd:YAG laser system and pumping with the triple harmonic at 355 nm, and the temperature dependence of the CARS intensity, mainly determined by the Boltzmann population difference factor, which lowers the signal intensity more severely at elevated temperatures in rotational CARS than in vibrational CARS.

The first demonstration of rotational CARS experiments was performed by Barrett,[10] who reported measurements on the $J = 3 \rightarrow 5$ transition in H_2. However, since the Raman shift for this transition is over one thousand wavenumbers, simple dichroic mirrors could

The authors are with Lund Institute of Technology, Combustion Center, P.O. Box 118, S-221, 00 Lund, Sweden.

Received 26 September 1988.
0003-6935/89/153206-14$02.00/0.

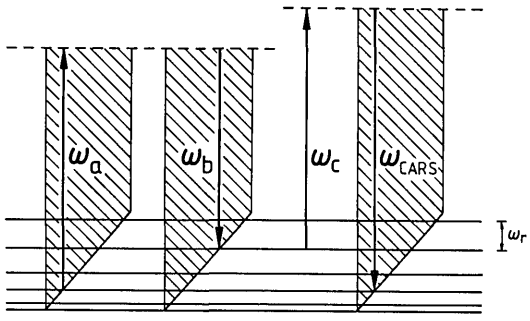

Fig. 1. Energy level diagram describing the rotational dual broadband CARS technique. The three lasers involved in the CARS generating process are in this paper generally denoted *a*, *b*, and *c* (from left to right in the figure). For RDBC, lasers *a* and *b* are broadband (~100 cm^{-1}) and laser *c* is narrowband (~1 cm^{-1}).

be used to spectrally isolate the CARS beam. The first application of rotational CARS for probing small Raman shifts was demonstrated by Beattie *et al.*[11] in a four-color technique. Small Raman shifts were later probed with rotational CARS using a phase mismatched configuration to separate the CARS beam[12] and by polarization suppression of the strong primary laser beams.[13] However, the introduction of a 3-D phase matching configuration, the so-called folded BOXCARS technique,[14] was something of a breakthrough for rotational CARS, since it permitted spatial isolation of the CARS beam and strong rejection of the laser beams by comparatively simple means. This technique was later used for temperature measurements both in cold gases[15] and in flames.[16]

As mentioned above, most rotational CARS experiments performed so far have been carried out using a Nd:YAG based laser system, which has meant that the 355-nm beam has been used to pump a dye laser with a coumarin dye. Since this dye suffers from low efficiency, short lifetime, and large shot-to-shot spectral irregularities, the rotationl CARS technique has been hampered. There have also been reports on rotational CARS using an excimer based laser system,[17] which is, however, subject to the extra complexity of using two independent dye lasers. One potential way of reducing some of the drawbacks with rotational CARS, as mentioned above, is to use dual broadband techniques, originally demonstrated in vibrational CARS[18] and recently also for the generation of rotational CARS spectra.[19,20] Although it is not until recently that the rotational dual broadband CARS technique was demonstrated, the concept was proposed already in 1979 by Yuratich.[21] Briefly, this technique utilizes two broadband ($\simeq$100-cm^{-1}) dye laser beams originating from one or two dye lasers and one pump laser beam, as illustrated in Fig. 1. Each rotational transition is driven by multiple pairs of laser frequencies, where each of the two components within each pair comes from a separate dye laser beam. Once the transition is excited, photons from the pump laser are scattered off the coherently vibrating molecules forming a spectrum at the Stokes (CSRS) and anti-Stokes (CARS) rotational Raman frequencies around the pump laser frequency. The three lasers involved in the CARS generating process are, in this paper, generally denoted *a*, *b*, and *c* (from left to right).

One advantage with this technique, when a Nd:YAG based laser system is used, is thus that very stable dyes, e.g., rhodamines, can be used. Another advantage with this technique is that, potentially, a spectral averaging effect could be achieved, even on a single-shot basis, since each CARS component is generated from essentially all dye laser frequency components. Several authors have suggested that this may result in dual broadband techniques having particularly good signal-to-noise ratios.[18–20,22,23] In Ref. 20 some quantitative support for such thoughts was given. It is generally believed that noise (spectral or temporal) in the laser radiation limits the accuracy of CARS thermometry.[24–27] Thus noise properties of, in particular, different experimental approaches to vibrational CARS, have been the subject of considerable interest lately (see, e.g., Refs. 22–25, 28, and 29). As an aid of finding an experimental approach to CARS with good-signal-to-noise ratio (i.e., good temperature accuracy), a model for calculating the best signal-to-noise ratio theoretically obtainable for different approaches to CARS has been developed.[30]

In this study we have measured temperature accuracies and signal intensities in a room temperature nitrogen flow and in a flame environment for conventional vibrational CARS and for different experimental configurations for rotational CARS. The evaluated temperature accuracies are compared to theoretical calculations of the obtainable signal-to-noise ratios in Ref. 30, and some general aspects on how multimode laser radiation may affect the accuracy are discussed. This paper also contains a description of the computer code for generating rotational CARS spectra, and the potential for the application of rotational CARS techniques to diagnostics in sooty flames, at high pressure (up to 40 atm), and for multiple species detection is discussed.

II. Theory

The theory section consists of two parts. First the computer routines for determining the temperature from rotational CARS spectra are described. Then a brief summary of how laser statistics influence the signal-to-noise ratio in broadband CARS, and thereby also the temperature accuracy in CARS thermometry, is given. In particular, an intuitive semiquantitative picture for estimating the noise in the dual broadband techniques where two broadband lasers are used in the CARS process is presented.

A. Computer Code

The rotational CARS code used in this work is a modification of a code for vibrational CARS which is described in Ref. 31 and follows the approach of Hall and others in Refs. 32–35. A detailed description of the changes that have been made in order to use the code for rotational CARS is given in Ref. 36. The main differences between the rotational and the vibrational codes are given below together with some excerpts from the general theory for rotational CARS.

The anti-Stokes intensity (I_{as}) as a function of the anti-Stokes frequency (ω_{as}) can be expressed as (see, e.g., Ref. 21)

$$I_{as}(\omega_{as}) = \iiint |\chi^{(3)}(\omega_{as},\omega_a,\omega_b,\omega_c)|^2 I_a(\omega_a) \times I_b(\omega_b) I_c(\omega_c) \delta(\omega_a - \omega_b + \omega_c - \omega_{as}) d\omega_a d\omega_b d\omega_c,$$

where $I_x(\omega_x)$ is the intensity of laser x at frequency ω_x, $\delta(\ )$ is the Dirac delta function, $\chi^{(3)}$ is the third-order susceptibility which, for our purposes, can be appropriately expressed as $\chi^{(3)} = \chi_R^{(3)} + \chi_{NR}^{(3)}$, where $\chi_{NR}^{(3)}$, the nonresonant third-order susceptibility, can be regarded as a frequency independent constant.

The resonant contribution $\chi_R^{(3)}$ is given by

$$\chi_R(\omega) = \frac{N}{\hbar} \sum_J \frac{3}{45} \cdot \frac{b_J^{J'} F(J) \beta_v^2 \Delta\rho_{JJ'}}{(\omega_a - \omega_b - \omega_J) - i\Gamma_J/2} \equiv \sum_J \frac{a_J}{\omega_a - \omega_b - \omega_J - \frac{i\Gamma_J}{2}},$$

where the summation runs over all Raman resonances (J) in the molecular species probed, $\hbar$ is Planck's constant/2π, ω_J is the Raman shift in wavenumbers, Γ_J is the corresponding rotational Raman linewidth (FWHM), N is the molecular number density, and $\Delta\rho_{JJ'}$ is the normalized population difference between the states J and $J+2$, more explicitly given by

$$\Delta\rho_{JJ'} = (2J+1) g_J \exp\{-[E(v,J+2) - E(v,J)]/kT\}/Q$$

for the O branch (CSRS) and

$$\Delta\rho_{JJ'} = (2J+1) g_J \exp\{-[E(v,J) - E(v,J+2)]/kT\}/Q$$

for the S branch (CARS). Q is the partition function and g_J is a nuclear J-dependent spin factor. Numerical values for χ_{NR} have been taken from Rosasco and Hurst.[37] $F(J)$ is a centrifugal correction factor[38,39] which has been approximated by unity.

Here $b_J^{J'}$ is the Placzek-Teller coefficient and is given by

$$b_J^{J+2} = \frac{3(J+1)(J+2)}{2(2J+1)(2J+3)},$$

for the O branch (CSRS) and

$$b_J^{J-2} = \frac{3J(J-1)}{2(2J+1)(2J-1)},$$

for the S branch (CARS). The rotational Raman linewidths, Γ_J, have been set equal to the vibrational Raman linewidths. β_v is the polarizability anisotropy and consists of a vibrationally independent part (β_e) with anharmonic correction terms:

$$\beta_v = \beta_e + \beta_e' \langle r - r_e \rangle_v + 0.5\beta_e'' \langle r - r_e \rangle_v^2. \quad (1)$$

The quantities in Eq. (1) are defined in Ref. 38 where numerical values are also given for N_2, O_2, and H_2, and CO. Raman linewidths and gain in N_2 as a function of temperature density and wavelength have also been investigated more recently.[40,41]

The expression given by Yueh and Beiting for integration over the laser profiles[42,43] have been extended to include the case for three different lasers yielding (using a notation consistent with Ref. 42)

$$I_{as}(\omega_{as}) = A(\chi_{NR}^2 + B + 2C),$$

where

$$A = \frac{\exp[-(\delta_{as}/\tilde{\gamma}_{2d})^2]}{\sqrt{\pi}\tilde{\gamma}_{2d}},$$

$$B = -\frac{2\sqrt{\pi}\tilde{\gamma}_{2d}}{\tilde{\gamma}_3\tilde{\gamma}_d} \chi_{NR} \sum_j a_j \operatorname{Im}[w(z_{3j})],$$

$$C = -\frac{\sqrt{\pi}\tilde{\gamma}_{2d}}{2\tilde{\gamma}_3\tilde{\gamma}_d} \sum_{j,k} a_j a_k \operatorname{Im}\left[\frac{w(z_{3j}) + w^*(z_{3k})}{\Delta_{kj} + i(\gamma_k + \gamma_j)}\right],$$

$\delta_{as} = \omega_{as} - \omega_{as}^0$,

$\Delta_j = \Omega_j - (\omega_a^0 - \omega_b^0)$,

$\Delta_{kj} = \Delta_k - \Delta_j$,

$\Omega_j \equiv$ the Raman shift,

$\omega_{as}^0 = \omega_a^0 - \omega_b^0 + \omega_c^0$,

$\omega_{as}^0, \omega_a^0, \omega_b^0, \omega_c^0 \equiv$ anti-Stokes and laser center frequencies, respectively,

$w(z) \equiv$ the complex error function

$$= \exp(-z^2)\left[1 + \frac{2i}{\sqrt{\pi}} \int_0^z \exp(t^2) dt\right]$$

$$= \frac{i}{\pi} \int_{-\infty}^{\infty} \frac{\exp(-t^2)}{z - t} dt, \qquad \operatorname{Im}(z) > 0$$

$$= z_{3j} = (\tilde{\gamma}_3\tilde{\gamma}_d/\tilde{\gamma}_{2d})^{-1}\left[\left(\frac{\gamma_d}{\gamma_{2d}}\right)^2 \delta_{as} - \Delta_j + i\gamma_j\right],$$

$\gamma_d = (\gamma_a^2 + \gamma_b^2)^{1/2}$,

$\gamma_{2d} = \sqrt{\gamma_d^2 + \gamma_c^2}$

$\tilde{\gamma} = \gamma/\sqrt{\ln 2}$,

$\gamma_a, \gamma_b, \gamma_c, \gamma_j \equiv$ laser and Raman linewidths (HWHM), respectively.

In particular, by letting $\gamma_a = \gamma_b$ and $\omega_a^0 = \omega_b^0$ the expression above is valid for rotational dual broadband CARS using one dye laser. For conventional rotational CARS a cross coherence contribution[44,45] must be taken into account. We have, however, used the Yuratich form[21] for the convolution also in conventional rotational CARS. This can, as far as we understand, only significantly affect the precision but not the accuracy in the temperature measurements for this approach. The computer code described above is used to generate sets of theoretical spectra at various temperatures which are then fitted to experimental spectra following the outline in Ref. 34. In Fig. 2 computer-

generated rotational CARS spectra of N_2 for temperatures of 300, 1300, and 2300 K are shown, demonstrating the population of higher rotational levels at increased temperatures.

The fitting program minimizes the quantity

$$\sum_{l=1}^{N}\left[\frac{I_{as}^{th}(\omega_l)}{\frac{1}{N}\sum_{k=1}^{N} I_{as}^{th}(\omega_k)}-\frac{I_{as}^{\exp}(\omega_l)}{\frac{1}{N}\sum_{k=1}^{N} I_{as}^{\exp}(\omega_k)}\right]^2. \quad (2)$$

Thus the model is only sensitive to the spectral shape of the CARS signal and not to temperature-dependent changes in the overall CARS intensity. This is further discussed in Ref. 31. $\{\omega_1\}$ is a set of equally spaced frequency points, and $I_{as}^{th}(\omega_1)$ and $I_{as}^{\exp}(\omega_1)$ are the intensities of the computer synthesized and experimental spectra at frequency ω_1, respectively. One or more of the parameters, temperature, concentration, OMA dispersion, and absolute frequency of the spectra can be fitted. Alternatively, the program can utilize the integrated Raman line intensities to determine the temperature. In this case $I_{as}(\omega_1)$ in Eq. (2) is exchanged for $I_A(J)$, where $I_A(J)$ is the integrated CARS intensity of the Raman transition between the rotational levels $J-1$ and $J+1$ and the summations in Eq. (2) are performed over all Raman lines J.

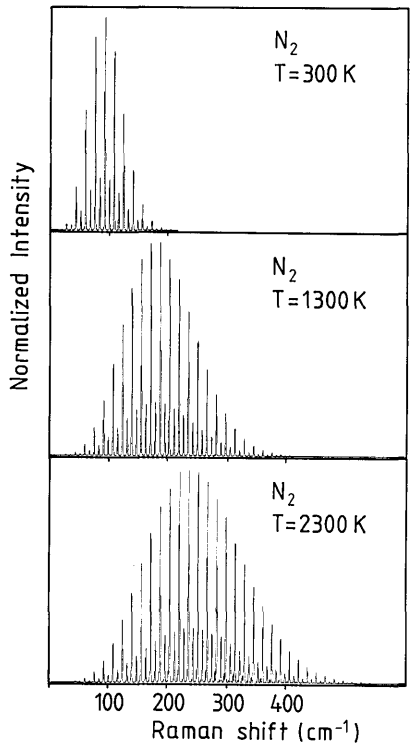

Fig. 2. Theoretical rotational CARS spectra of N_2 at temperatures of 300, 1300, and 2300 K.

B. Influence of Laser Statistics on Noise in Broadband CARS

Stochastic fluctuations in the laser mode amplitudes and laser mode phases will influence the signal-to-noise ratio and thereby also the temperature accuracy in single-shot CARS thermometry differently for different experimental approaches.[22–24,28,30] A quantitative analytical analysis of this issue is tractable if the individual laser mode amplitudes and phases are assumed to be statistically independent, if their variation with time during the laser pulse is neglected, and if the phases are assumed to be randomly distributed in the interval $[0,2\pi]$.[30] An intuitive semiquantitative picture of how the stochastic laser mode amplitudes affect the noise is given in Ref. 23. [In this section, noise is from now on defined as is conventionally done in broadband CARS thermometry,[25,28,29] i.e., essentially as $\sigma(I_{as})/E(I_{as})$, where $\sigma(x)$ and $E(x)$ are the standard deviation and expected value of x, respectively.] One of the main arguments in Ref. 23 was that, when considering the CARS signal within a given spectral interval, the noise contribution from stochastic mode amplitude fluctuations in a laser was inversely proportional to the square root of the number of modes from that laser contributing to the signal. The same argument, supported by experimental material, was also presented by Snelling *et al.*[22] The intuitive argument above agreed with the results obtained in the theoretically more rigorous treatment in Ref. 30. In Ref. 30 it was also pointed out that in the dual broadband techniques it is not the shot-to-shot fluctuations in the laser mode amplitudes but instead the shot-to-shot fluctuations in the laser mode phases which cause the noise. Since we have used dual broadband techniques for CARS thermometry in this work we wish to complement the previously published material on the influence of laser statistics on noise in broadband CARS by giving an intuitive semiquantitative picture of the noise contribution from stochastic laser mode phases.

Consider a mode k of an electromagnetic field, which can be written as $E_k = e_k \exp[i(\omega_k t + \phi_k)]$, where t is time, and e_k, ω_k, and ϕ_k are the amplitude, frequency, and phase of mode k, respectively. The phases are chosen such that the mode amplitudes are real.

The total intensity (I_0) from a field with two modes (1 and 2) is given by

$$I_0 = |E_1 + E_2|^2 = e_1^2 + e_2^2 + 2e_1e_2\cos[(\omega_1-\omega_2)t + \phi_1 - \phi_2]. \quad (3)$$

The noise due to shot-to-shot fluctuations in the term e_1^2 (e_2^2) is considered to arise from mode intensity fluctuations in mode 1 (2) and the noise due to shot-to-shot fluctuations in the cross term $2e_1e_2\cos[(\omega_1-\omega_2)t + \phi_1 - \phi_2]$ is considered to arise from phase fluctuations. Clearly also mode amplitude fluctuations will affect this term but to a smaller extent. In contrast to the two first terms (e_1^2,e_2^2) the average intensity contribution from several shots is zero for the cross term.

We choose to denote the first two terms as coherent terms and the cross term as an incoherent term. We furthermore claim that an approximate value of the noise contribution from stochastic phases is given by the ratio $\sqrt{N_{IC}}/N_C$, where $N_{IC}(N_C)$ are the number of incoherent (coherent) terms contributing to the signal. All incoherent terms will not generally contribute to the signal. This is so because the integrated anti-

Stokes signal is observed only during a limited time T, where T is the duration of the anti-Stokes pulse, typically of the order of 10 ns. If $(\omega_1 - \omega_2)T \gg 2\pi$ the cross term will only give a negligible contribution to the signal (regardless of what value the phases ϕ_1 and ϕ_2 may have). Thus to count a cross term as contributing we demand (quite arbitrarily) that the frequency difference in the argument should be smaller that $1/T$. We illustrate the approach with a specific example where there are two broadband dye lasers, lasers a and b in Fig. 1, with bandwidths Γ_a and Γ_b ($\Gamma_a < \Gamma_b$), mode spacings Ω_a and Ω_b and a single-mode laser as laser c. Further, it is assumed that the signal from a Raman resonance with width Γ_r is observed, that W, the detection system instrument function, is much larger than Γ_r and, finally, that the inverse duration of the anti-Stokes pulse is smaller than the laser mode spacings. To obtain the number of contributing coherent terms it is noted that any mode can be chosen from laser a but then only Γ_r/Ω_b modes from laser b to obtain the signal. Thus

$$N_c = \frac{\Gamma_a}{\Omega_a} \cdot \frac{\Gamma_r}{\Omega_b} .$$

To obtain the number of contributing incoherent terms any mode from laser a and again Γ_r/Ω_b modes from laser b may be chosen. The anti-Stokes electric field mode constructed from these two modes and the mode from laser c may then beat against other anti-Stokes modes which are constructed by first taking any mode from laser a and then one of $1/(T\Omega_b)$ possible modes from laser b. Thus

$$N_{IC} = \frac{\Gamma_a}{\Omega_a} \cdot \frac{\Gamma_r}{\Omega_b} \cdot \frac{\Gamma_a}{\Omega_a} \cdot \frac{1}{T\Omega_b} ,$$

$$\text{noise} = \frac{\sqrt{N_{IC}}}{N_C} = \frac{1}{\sqrt{T\Gamma_r}} ,$$

which is consistent with the result from the more detailed calculations in Ref. 30. The noise term above also occurs in Eqs. (4b) and (4c) in Sec. V of this paper. For the measurements presented in this paper one must calculate the number of incoherent terms between all pairs of modes of the multimode lasers while taking a specific mode from the third laser. (The calculation above corresponds to the case when taking a specific mode from laser c.) Then the number of incoherent terms where none of the lasers contributes with the same mode to the anti-Stokes modes beating against each other must also be calculated. Finally all these noise terms (including the mode amplitude fluctuation contributions) are added in quadrature yielding expressions such as those in Eq. (4) (compare also to Refs. 30 and 46).

III. Experimental Approach

Four different experimental approaches to rotational CARS were investigated, together with conventional vibrational CARS, by recording 105 single-shot spectra at both room temperature and flame temperature. The room temperature spectra were measured in a flow

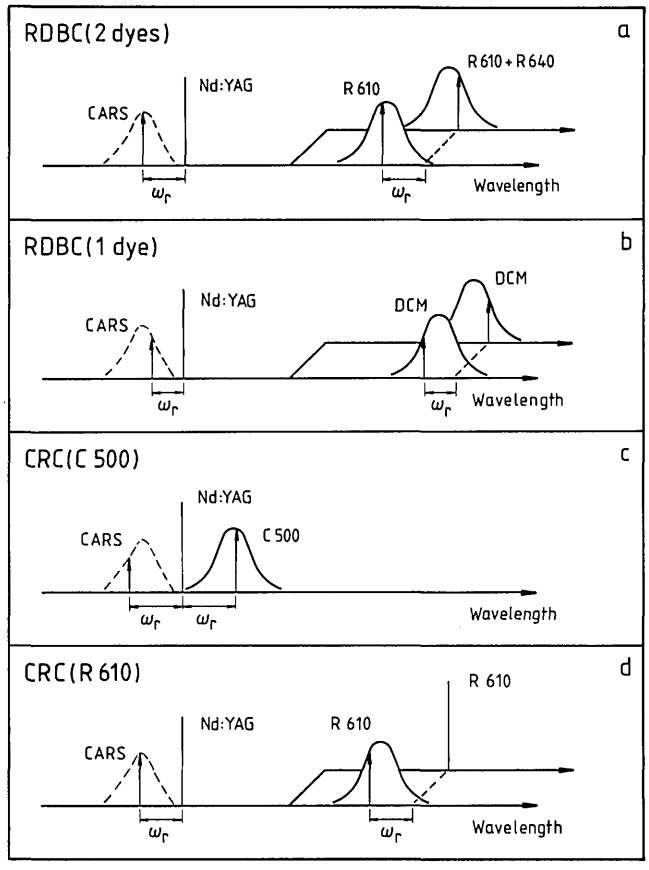

Fig. 3. Schematic representation of the different rotational CARS approaches that were investigated: (a) rotational dual broadband CARS using two different dye lasers, RDBC(2 dyes); (b) rotational dual broadband CARS using one single dye laser, RDBC(1 dye); (c) conventional rotational CARS using coumarin 500 as dye, CRC(C 500); (d) conventional rotational CARS using rhodamine 610, CRC(R 610).

of nitrogen at 295 ± 1 K and the flame spectra at a height of 8 mm above a water-cooled porous-plug burner (d = 40 mm) in the burnt gases of a premixed methane/air flame, with a C/O ratio of 0.34. The N_2 mole fraction in the flame was 0.68. The use of a flat flame on a porous-plug burner as a hot gas generator together with very accurate mass flow controllers is expected to give a very reproducible temperature in the burnt gas region.

To compensate for the difference in efficiency in the CARS generating process at different wavelengths, caused by the limited dye laser bandwidth, the resonant CARS spectra were divided by a corresponding nonresonant CARS spectrum. This nonresonant spectrum was generated in a flow of argon at atmospheric pressure and room temperature. The peak signal strength of the nonresonant spectrum when using the rotational dual broadband technique with DCM as dye was around 6000 counts for each laser shot.

Of the four rotational CARS approaches used, two were dual broadband approaches and two conventional CARS approaches, as illustrated in Fig. 3. In the

first, rotational dual broadband CARS using two dyes, RDBC(2 dyes), the rotational Raman transitions were coherently excited by multiple pairs of photons, one from each dye laser beam before coupling to photons at 532 nm. The other rotational dual broadband technique only utilizes one dye, RDBC(1 dye). In these experiments DCM or R 610 were used and will be referred to as RDBC(DCM) and RDBC(R 610). For RDBC(1 dye) the rotational Raman transitions were again excited by multiple pairs of photons, one photon from each dye laser beam which here originated from the same dye laser whose output beam had been split into two. The last two techniques are conventional rotational CARS techniques where the rotational Raman transitions are excited between a narrowband laser and a broadband dye laser, either between the Nd:YAG laser beam at 532 nm and coumarin 500 or between a narrowband laser at 592 nm and rhodamine 610 and they will be referred to as CRC(C 500) and CRC(R 610). In CRC(C 500) only one dye laser is used and a dye laser photon is combined with two Nd:YAG laser photons to yield a CARS photon. In general discussions this technique will be referred to as CRC(1 dye), while CRC(R 610) utilizes two dye lasers, one broadband and one narrowband, and will be referred to as CRC(2 dyes). The techniques are described one by one and the different experimental features are presented.

A. RDBC(2 dyes)

The experimental setup for this technique is shown in Fig. 4. The frequency doubled output energy from the Nd:YAG laser (Quantel YG-581 C) at 532 nm was ~550 mJ/pulse with a pulse duration of ~10 ns. Thirty percent of this pumped a Quanta-Ray PDL-1 dye laser with a dye mixture of rhodamine 610 and rhodamine 640, 55% was used to pump the dye oscillator and dye amplifier of a Quantel TDL-50 dye laser, and the rest was used in the CARS generating process. The residual infrared radiation from the doubling process was frequency doubled in a second crystal yielding an output energy of ~110 mJ/pulse at 532 nm which pumped the preamplifier stage of the Quantel dye laser. (In a first setup the frequency doubled beam from the residual infrared radiation was used in the CARS generating process. However, since the beam profile appeared to be of rather low quality, the CARS signal intensity was anticipated to be lower than that with the experimental setup described above.) The broadband profile of R 610 peaked at 588 nm, while the mixture of R 610 and R 640 was tuned, by changing the dye concentration, to a wavelength where the wavelength difference between the peaks of the dye laser profiles yielded maximum rotational CARS intensity for the examined molecule at the probed temperature. The three laser beams were adjusted by telescopes to the same beam diameter (d = 4 mm) and arranged in a BOXCARS setup with a focusing lens of f = 300 mm. The Nd:YAG laser beam and the dye laser beam with the spectral profile at the longer wavelength were positioned nearly on top of each other. In this configuration the CARS signal is favored compared with the CSRS signal. The CARS signal was separated from the dye laser radiation with dichroic mirrors and colored glass filters and focused with an f = 150-mm lens onto the slit of a 1-m Jobin-Yvon spectrometer. The grating, 600 rules/mm and blaze 2.5 μm, was used in the fourth order with a dispersion of 10 cm^{-1}/mm. The detector was an intensified diode array with 1024 elements connected to an optical multichannel analyzer (OMA III, EG&G PARC). The signal strengths at room temperature and flame temperature for the different rotational CARS approaches are given in Table I together with the laser pulse energies used for CARS generation. It can be seen that with our experimental setup, the techniques which require pumping of two dye lasers do not have the capability of generating as high signals as the RDBC(1 dye) technique which only requires pumping of one dye laser, although theoretically they should give about the same intensity. All rotational CARS techniques except CRC(C 500) were used in the planar BOXCARS approach, where the distance between the incoming laser beams was kept small (center-to-center distance of 6–7 mm) to obtain as high signal strength as possible.

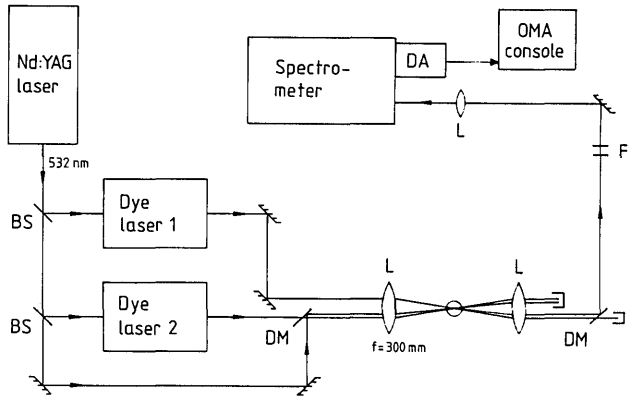

Fig. 4. Experimental setup used in the rotational dual broadband CARS technique utilizing two broadband dye laser beams, RDBC(2 dyes): BS = beam splitter; DM = dichroic mirror; DA = diode array; L = lens; and F = filters.

Table I. Pulse Energies for the Primary Laser Beams and the Resulting Experimental Peak Signal Strength in Room Temperature Nitrogen and at Flame Temperatures ($T \cong$ 1800 K) for the Different Rotational CARS Techniques

ω_a ω_b ω_c	Pulse energy (mJ)			Peak signal strength (counts)	
	ω_a	ω_b	ω_c	N_2, 1 atm T=295 K	Flame, 1 atm T≈1800 K
RDBC(DCM)	33	33	57	$5 \cdot 10^6$	$3 \cdot 10^3$
RDBC(R 610)	51	51	57	$2 \cdot 10^7$	$3 \cdot 10^3$
RDBC(2 dyes)	33	45	18	$4 \cdot 10^5$	$5 \cdot 10^2$
CRC(R 610)	33	20	18	$1.5 \cdot 10^5$	$4 \cdot 10^2$
CRC(C 500)	62	9	80	$1 \cdot 10^6$	$6 \cdot 10^2$

B. RDBC(1 dye)

For this technique all the Nd:YAG laser pulse energy was directed to the Quantel TDL-50 dye laser in the same manner as described for RDBC(2 dyes), to generate as high broadband pulse energy as possible. Two different dyes were used, DCM with a FWHM of ~305 cm^{-1} and R 610 with a FWHM of ~145 cm^{-1}. In this technique the dye laser beam was split into two before being combined with the 532-nm beam in a BOXCARS configuration. Since the dye laser profile has a finite width, the efficiency in the generation of the signal at larger Raman shifts will be limited. In Fig. 5(a) the nonresonant spectra from DCM and R 610 are shown and in Fig. 5(b) a flame spectrum generated by RDBC(DCM), divided by the corresponding nonresonant CARS spectrum, is presented. It is thus clearly shown that RDBC(R 610) is not as suitable for generation of a complete flame spectra as RDBC(DCM) since the FWHM for the nonresonant spectrum from R 610 was 205 cm^{-1} and the strongest transitions occur for Raman shifts around 200 cm^{-1} at flame temperatures. The FWHM for the nonresonant spectrum of DCM is 430 cm^{-1}. In the flame spectrum shown in Fig. 5(b), essentially only contributions from N_2 molecules are seen.

High signal strengths were registered for this technique both at room temperature and flame temperature. Peak single-shot signal strengths at a flame temperature of 3000 counts were registered for both RDBC(DCM) and RDBC(R 610), as presented in Table I. However, as illustrated in Fig. 5(a), the RDBC(R 610) technique strongly favors low Raman shifts and thus limits the number of rotational Raman lines which can be used to evaluate the temperature. In Fig. 6 both a single-shot spectrum and an averaged spectrum over 100 shots from a flame using RDBC(DCM) are shown, together with the difference between the experimental and the theoretical spectrum for the best fit.

For RDBC(DCM) all involved laser pulse energies were higher than 30 mJ. To check that no effects of too high laser fluence were present, e.g., due to saturation, a test was made where spectra were recorded both with incident pulse energies in the dye laser beam and the Nd:YAG beam of 66 and 57 mJ, respectively, and with 12 and 10 mJ, respectively. Since these spectra were nearly identical, it was concluded that there were no such effects.

A non resonant CARS contribution to the flame spectra was observed, which was seen only when the three involved laser beams were present. However, when the spectra were divided by a nonresonant CARS spectrum, the result was a constant background which was of little importance when applying curve fitting to the spectra (see Sec. IV).

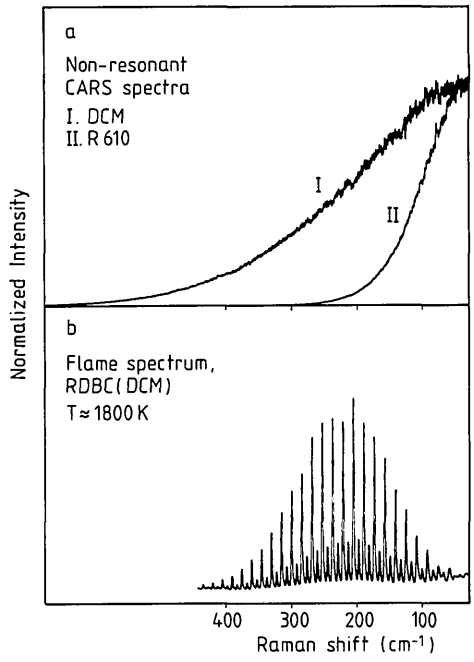

Fig. 5. (a) Nonresonant CARS spectra using the dyes DCM and rhodamine 610. (b) Flame spectrum generated using rotational dual broadband CARS with DCM dye, RDBC(DCM), corrected for the limited dye laser bandwidth. The frequency scale is the same in (a) and (b).

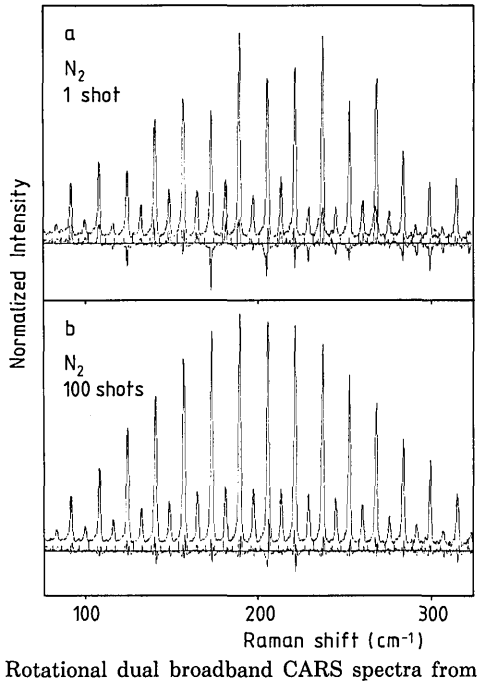

Fig. 6. Rotational dual broadband CARS spectra from a flame using DCM dye: (a) single shot and (b) 100 shots. Below each spectrum the difference between the experimental spectrum and the theoretical spectrum is shown.

C. CRC(C 500)

This is an approach which has been frequently used for rotational CARS generation but, as described in Sec. I, it suffers from several experimental disadvantages. For the CRC(C 500) technique the folded BOXCARS approach had to be used to prevent green light at 532 nm from reaching the detector, and with the dichroic mirrors available it was not possible to keep the distance between the laser beams as small as

in the BOXCARS technique, which resulted in a loss in signal strength.

Comparing our single-shot spectra, after compensation for the differences in laser power, with the quality of the spectrum given in Ref. 16, we would expect a much higher CARS signal with this technique. The reason for this discrepancy is not known, however, parameters such as beam quality, different pulse lengths, and a more wavelength-optimized dye laser may partly explain the discrepancy.

D. CRC(R 610)

The difference between this technique and RDBC(2 dyes) is that the Quanta-Ray laser is run in the narrowband mode instead of in the broadband mode. The reason for exploring this technique was that, to determine if the dual broadband techniques from the noise characteristics point of view were different from the conventional rotational CARS techniques, it seemed appropriate to make comparisons with the conventional CARS approach using not only the more unstable coumarin but also a rhodamine dye.

E. Vibrational CARS

The vibrational CARS technique, used in the BOXCARS approach, was also investigated concerning accuracies in single-shot temperature determination at room temperature and flame temperature. It was also used to determine the flame temperature since the vibrational CARS computer code has been checked against a temperature-stabilized oven which has not yet been done for the rotational CARS computer code.

IV. Analyses and Results

After being captured by the OMA each experimental spectrum is represented as an array with 1024 elements. The intensity of element K in spectrum number i is denoted $I_i(K)$. For each set of 105 spectra an average spectrum is first calculated

$$I^{ave}(K) = \frac{1}{105}\sum_{i=1}^{105} I_i(K).$$

For this average spectrum, temperature, a calibration frequency for an arbitrarily chosen diode and the detection system dispersion are determined by a fit to theoretical spectra. The concentration has not been fitted. The room-temperature measurements were carried out in a flow of pure nitrogen, and for the flame temperature measurements concentrations calculated from the mass flow measurements mentioned in the previous section were used. The nonresonant susceptibility was scaled a factor of 1.2 with respect to the nitrogen value.[34,47,48] The dispersion calculated from the average spectrum is used as a fixed parameter when evaluating the individual single-shot spectra. Empirically, it was observed that the spectra may change position slightly on the diode array from shot to shot.[31] Thus the calibration frequency is fitted separately for each spectrum. The value obtained from the average spectrum is used as a starting value. The initial value for the temperature was (arbitrarily) chosen to be 1700 K. The initial values of calibration frequency and temperature do not influence the final temperature. However, a good initial value for the calibration frequency decreases the computer time needed to fit the spectra. For each set of spectra the average temperature (T^{ave}) and the standard deviation (σ_T) have been calculated. Fitting a full spectrum typically required ~60 CPU seconds on a Nord 500 computer (slightly higher CPU capacity than a Vax 8200). If, as mentioned in Sec. II, only the integrated Raman line areas were used instead of the full spectral signature to obtain a temperature, evaluation of a full set of 105 spectra only required ~20 CPU seconds. This method only gave about a 50% higher standard deviation but the average temperature was more sensitive to variations in the background intensity and appeared to be less reliable. However, for most cases the mean temperature from curve and area fitting still agreed within 50 K at flame temperatures. As will be discussed in the next section, the difference in average temperature for sets recorded with different techniques generally differed by more than this. There may be alternative ways to reduce the computation time. In Refs. 49 and 50 the authors suggested a fast Fourier transform method as a possibility for rapid determination of rotational temperatures.

The experimental values for the relative single-shot temperature uncertainty ($100 \cdot \sigma_T/T^{ave}$) for room temperature and flame spectra obtained with the different experimental approaches are given in Table II. For the flame measurements the results from two sets of RDBC(DCM) spectra recorded on two different occasions are given. We believe that the difference in relative accuracy between these two sets reflects the accuracy of the values in Table II. Thus the relative uncertainties are assumed to be correct to within 10–20% (if this is a correct assumption then strictly only the first digit for the values in Table II is significant). Further, due to lack of signal strength for the CRC and RDBC(2 dyes) techniques, the count rate at the detector was not the same for all flame measurements and also because of the difference in spectral width for the different dyes the spectral interval of the CARS spec-

Table II. $100 \cdot \sigma(T)/T^{Ave}$ is Given, Where T^{Ave} is the Average Temperature from 105 Single-Shot Measurements and $\sigma(T)$ is the Standard Deviation in the Single-Shot Temperatures

Experimental approach	Room-temperature nitrogen	Flame
RDBC(2 dyes)	4.9	4.7
RDBC(DCM)	4.7	5.6
RDBC(DCM) *	-	6.3
RDBC(R 610)	4.2	3.8
CRC(C 500)	5.7	14
CRC(R 610)	5.1	7.2
Vibrational CARS	10.2	2.7

* A second set with 105 DCM flame spectra was recorded.

tra that could be used for determining the temperature differed between the different techniques. The flame results are thus appropriate for determining which technique is most accurate for flame measurements but less well suited for general evaluation regarding noise properties. We note though that the accuracy was not limited by shot noise in any of the measurements. Based on Table II and the discussion above, it can be concluded that rotational CARS is more accurate than vibrational CARS at room temperature and vice versa at flame temperature and, further, that CRC(C 500) (i.e., the approach which has normally been used for rotational CARS) is not well suited for flame temperature measurements. [The coumarin dye is preferably used to generate CSRS spectra since it has its peak value shifted toward higher frequencies than the Nd:YAG second harmonic. However, CSRS spectra recorded with CRC(C 500) did not have a better temperature accuracy than the CARS spectra.] Also, on inspection of Table II the impression is that the RDBC approaches in general have lower temperature standard deviations than the CRC approaches, compare, for example, RDBC(R 610) and CRC(R 610). This will be more extensively discussed in the next section in connection with theoretical estimates of the accuracy for the different methods.

V. Discussion

One aim of the present work was to investigate whether the RDBC techniques show lower noise properties than the CRC techniques. There were reasons to believe that this could be the case since both experimental results[20] and theoretical calculations[30] have indicated lower noise for the RDBC techniques. In Ref. 20 the nonshot noise part of the noise in nonresonant CARS spectra recorded with CRC(1 dye) [or actually vibrational CARS, however, using the model in Ref. 30 the theoretically calculated noise figures will be the same in CRC(1 dye) and vibrational CARS for a nonresonant spectrum] and RDBC was measured. While the noise in the RDBC spectra was about the same as the spectral noise in the dye laser ($\simeq 5\%$), the noise in the CRC spectra was a almost a factor of 2 higher. In Ref. 30 the noise-to-signal ratios (NSRs) for different experimental approaches to CARS were calculated assuming Gaussian laser statistics[51] (many independent modes) yielding slightly lower NSR for the RDBC techniques. Further, apart from determining which CARS technique is the most appropriate for accurate temperature determination, comparing the inaccuracy, or noise-to-signal ratio, in RDBC and CRC techniques is also interesting from a more fundamental point of view. The reason is, as pointed out in Ref. 30, that in the limiting cases where the narrowband laser(s) in RDBC and CRC is (are) single mode the noise in CRC is determined by the spectral noise (mode intensity fluctuations) in the broadband laser while the noise in the RDBC techniques is determined by the shot-to-shot variations in the laser mode phases. Observing the laser pulses with a spectral resolution sufficient to look at individual modes, shot-to-shot fluctuations in the laser mode phases would not affect the spectral intensity distribution but would show up as fluctuations in the temporal profile. Thus, in these limiting cases the temperature accuracy in CRC and RDBC can, to some extent, be thought of as being limited by spectral and temporal fluctuations in the broadband lasers, respectively. From the arguments above it is not surprising that the RDBC CARS noise in Ref. 20 could be as low as the dye laser spectral noise since this noise does not limit the accuracy of RDBC. The different noise origins for the CRC and RDBC techniques may become particularly interesting since it has recently been demonstrated that, using a suitable dye laser amplifier arrangement, it is possible to produce temporally smooth,[52] or alternatively, spectrally smooth[53] broadband dye laser pulses.

In the present investigation, the leading terms for the NSR due to the stochastic fluctuations of the laser radiation are[30,46]:

RDBC(1 dye)

$$\frac{1}{\sqrt{2}}\left[\frac{\sqrt{2\pi}}{T\Gamma_c}\sqrt{1+\frac{\Gamma_c^2}{W^2}}+\frac{1}{2\pi}\frac{\Omega_a}{\Gamma_r}\right]^{1/2}; \tag{4a}$$

RDBC(2 dyes) and CRC(2 dyes) (corresponds to DBC in Ref. 30)

$$\left[\frac{1}{\sqrt{2\pi}}\frac{\Omega_a}{\Gamma_a}+\frac{\sqrt{2\pi}}{T\Gamma_c}\sqrt{1+\frac{\Gamma_c^2}{W^2}}+\frac{1}{T\Gamma_r}\right]^{1/2}; \tag{4b}$$

CRC(1 dye), (corresponds to CC in Ref. 30)

$$\left[\frac{1}{\sqrt{2\pi}}\frac{\Omega_b}{\Gamma_a}+\frac{\sqrt{2\pi}}{T\Gamma_a}\left(\sqrt{1+\frac{\Gamma_a^2}{W^2}}+4\sqrt{1+\frac{\Gamma_a^2}{2W^2+\Gamma_a^2}}\right)+\frac{1}{T\Gamma_r}\right]^{1/2}; \tag{4c}$$

Ω_i and Γ_i are mode spacing and spectral width ($1/e$ Gaussian halfwidth) of the laser providing photon i in Fig. 1, W is the instrument function, T is the duration of the anti-Stokes pulse, and Γ_r is the width of the Raman resonance. The spectral widths can be converted to FWHM by multiplying by a factor of $2\sqrt{\ln 2}$. The values for our experimental configurations are given in Table III.

The expression above for RDBC(1 dye) differs from the one in Ref. 30, Appendix E, by a factor of $1/\sqrt{2}$. This is because the present expression is for uncorrelated beams while the expression in Ref. 30 is for correlated beams (In Ref. 46 it is described how the case of uncorrelated beams is taken into account for second harmonic generation. The procedure outlined there is directly applicable to the CARS calculations in Ref. 30.) The coherence length for the broadband dye laser beams is ~0.01 cm. Thus, unless special care is taken to ensure that the two dye laser beams travel the same distance before reaching the focal point, they will generally be uncorrelated. Also for CRC(1 dye) the question of correlated and uncorrelated beams must be considered. However, it turns out that the NSR is unaffected as long as the difference in propagation distance is less than the inverse of the Raman

linewidth ($\simeq 0.08$ cm^{-1}) which normally would be the case.

The first term in Eqs. (4b) and (4c) arises from mode intensity fluctuations while all other terms are interpreted as being caused by phase fluctuations. The reasons for this separation of the noise sources are discussed extensively in Ref. 30. One additional argument is that in the theoretical model both laser mode phases and laser mode amplitudes are assumed to be time independent during the generated pulse. Because of this the noise due to shot-to-shot variations of the mode intensities are independent of the duration of the detected pulse but the noise from mode beating terms will indeed have a $1/T$ dependence as seen in Eqs. (4a)–(4c). The last term in Eq. (4a) is a special case and this is also discussed in Ref. 30.

In Table IV the NSRs obtained from Eqs. (4a)–(4c) using the experimental values in Table III are given. To compare the obtained temperature accuracy with the calculated noise figures the theoretical values have all been multiplied by a common factor (0.4) such that the RDBC(2 dyes) figure is 4.8%. It is only meaningful to compare them in this way if the uncertainty in temperature is linear with the NSR. From the results of Snelling *et al.*[22] one may possibly infer that at least for vibrational CARS the temperature uncertainty does not appear to be a strongly nonlinear function of the NSR. Vibrational CARS is not included in Table IV. For conventional vibrational CARS Eqs. (4c) should be used to calculate the noise. The scaling factor will, however, most likely not be the same for vibrational and rotational CARS since, first, the resonances in vibrational CARS are not resolved and, second, the temperature is derived from the CARS signature in a different way.

As an example of how the calculated noise can be analyzed in terms of the discussion about different contributions to the noise above one may look at Eq. (4b) and Table IV. The only difference between the RDBC(2 dyes) and CRC(2 dyes) cases is the smaller bandwidth of laser *a*. With a bandwidth of 100 cm^{-1} the first term in Eq. (4b) is negligible but with a bandwidth of only 0.6 cm^{-1}, as in CRC, the first term makes a significant contribution to the NSR. That is, with only one broadband laser the spectral fluctuations in this laser start to contribute to the noise.

Apart from approximations in the theoretical model, uncertainties in the theoretical values are also due to insufficient knowledge of some of the experimental parameters in the measurements. In particular, this is the case for the spectral width of the Quanta Ray dye laser and the duration of the anti-Stokes pulse.

The general trends in Table II and IV are very similar. Both theoretical and experimental results indicate that the dual broadband techniques are more appropriate for accurate temperature measurements. However, with a 10% inaccuracy for both theoretical and experimental values definite statements regarding the agreement between theory and experiment or the best experimental method cannot be made.

In the field of rotational CARS there has been very little work directed toward the investigation of noise characteristics and temperature accuracy. In Refs. 14 and 15 conventional rotational CARS using a coumarin dye were investigated in that ten and twenty individual spectra were evaluated in terms of temperature accuracy at low and flame temperature, respectively, using a referencing technique. In those studies the standard deviations at room temperature and at flame temperature were found to be $\simeq 3.5$ (rms) and $\simeq 9\%$, respectively. In Ref. 17, where an excimer-based rotational CARS setup was used, a temperature standard deviation of $\sim 8\%$ was found at 700 K. If these values are compared with our values given in Table II for CRC(C 500), our values are seen to be higher. The main difference between our experiment and the ones in Refs. 14 and 15 is that we have not used any reference technique. However, as was pointed out in Ref. 23, referencing using a spectrograph with a resolution much lower than the Raman linewidth and a nonresonant gas, e.g. argon, may not (in particular if the pump laser is narrowband) improve the noise characteristics to any great extent. This has also been observed in vibrational CARS by Pealat *et al.*[26]

As mentioned earlier, the average temperature (T^{ave}) was calculated from each set of 105 spectra. The spread in T^{ave} between the sets was 3% for the room temperature spectra and as much as 12% for the flame temperature measurements. Since these experiments were performed with completely different

Table III. Experimental Values Used to Calculate Theoretical Noise-to-Signal Ratios from Eq. (4)[a]

	RDBC(1 dye)	RDBC(2 dyes)	CRC(2 dyes)	CRC(1 dye)
Ω_a	0.012	-	-	-
Ω_b	-	0.012	0.012	0.012
Γ_a	-	~100	0.6	0.4
Γ_c	0.4	0.4	0.4	-
W	0.6			
Γ_r	0.05			
T	$2\pi c \cdot 10$ ns = 600π cm			

[a] Ω_x and Γ_x are mode spacings and spectral widths (1/e Gaussian halfwidths) of laser x (subscripts refer to Fig. 1), W is the detection system instrument function, Γ_r is the width of the Raman resonance and T is the duration of the anti-Stokes pulse. All Γ:s and W:s can be converted to FWHM by multiplying by a factor $2\sqrt{\ln 2}$. All units are cm^{-1} except where otherwise stated. c is the speed of light.

Table IV. Theoretically Calculated Noise-to-Signal Ratios Scaled by a Factor of 0.4 for Comparison with the Temperature Accuracies in Table II

Experimental approach	Theoretically calculated noise-to-signal ratio
RDBC(2 dyes)	4.8
RDBC(1 dye)	5.6
CRC(2 dyes)	6.0
CRC(1 dye)	8.0

CRC(2 dyes) corresponds to CRC(R 610) in Table II and CRC(1 dye) corresponds to CRC(C 500).

experimental setups during a period of several months, great care was made to compare the results. However, the reason for the discrepancy between the average temperatures for the different techniques has not yet been solved although several experimental as well as theoretical potential sources of error have been considered such as spectral changes of the broadband dye laser, flame reproducibility and evaluation procedures. In the case of RDBC(R 610) the evaluated temperature was ~180 K too high compared to measurements using the vibrational CARS technique, which has yielded consistent values with thermocouple measurements in a heated oven.[31] This discrepancy might be explained by the fact that the limited dye laser bandwidth only permitted evaluation of a small number of rotational lines with large intensity differences both in the CARS spectrum and the nonresonant CARS spectrum. Such large intensity differences can lead to systematic errors in the evaluated temperature if the detector suffers from nonuniform gain characteristics as has been seen in vibrational CARS experiments.[31,54]

An advantage with the rotational dual broadband technique utilizing only one dye laser is that the results are insensitive to wavelength shifts of the broadband spectrum from the dye laser. This shift can be significant and has been observed in our laboratory in conventional vibrational CARS,[31] where the recording of a resonant spectrum must always be rapidly followed by the recording of a nonresonant spectrum to compensate for this wavelength drift. However, the dual broadband technique is sensitive to any pulse-to-pulse fluctuation in the halfwidth of the broadband dye laser, which would also be a potential source of error, e.g., in temperature measurements. We have made a brief investigation of the effect of width fluctuations on the rotational dual broadband technique. First, room temperature theoretical rotational CARS spectra generated with different dye laser linewidths were fitted to experimental nitrogen spectra using a DCM dye with a halfwidth of 318 cm^{-1}. As can be seen in Table V, a change in halfwidth by as much as 21.4% to 250 cm^{-1} gives a change in temperature of only 3.3%. To make an experimental comparison, the fluctuations in the dye laser halfwidth were measured for five different dyes and for a mixture of dyes, see Table VI. The result for DCM was a fluctuation of 4.3% (relative standard deviation) which, according to Table V, would give a temperature uncertainty of ~0.5%. Obviously the fluctuations in the dye laser halfwidth do not seem to be of any significance at room temperature. Of the other dyes investigated, rhodamine 590(R590), R610, R640, fluorescein, kiton red, and the dye mixture (R610 + R590), the dye mixture gave the largest fluctuations, 9.5%.

Although the primary aim of the experiments reported in this paper was to compare different rotational CARS techniques in terms of signal strength and temperature accuracy, we also investigated some additional properties of the technique.

So far only N_2 has been considered as a species for temperature measurements at flame temperatures. However, during the flame experiments we also detected high quality O_2 rotational CARS spectra from a lean methane/oxygen flame. It is attractive to use O_2 in rotational CARS since the rotational Raman cross section for this species is almost three times larger than that for N_2.[55]

A feature of rotational CARS, which has not been addressed in detail in the literature, is the possibility of multiple species detection using one single dye laser. The potential problem with spectral interference could be solved by using a spectrograph with high enough resolution. (Since the *f*/No. of a CARS spectrometer can be very large it would not pose any construction problems.) In Fig. 7 an example of a rotational CARS spectrum from a CO/O_2 diffusion flame is shown, where the peaks above $\simeq 100$ cm^{-1} come from CO molecules whereas the broadband wavelength distribution below $\simeq 100$ cm^{-1} is attributed to CO_2. This spectrum was recorded with the rotational dual broadband CARS technique using DCM as dye. An attractive application of rotational CARS would, for example, be to simultaneously measure oxidant, fuel, and some product which would be of great interest, e.g., in turbulent combustion.

Table V. Effects of Width Deviation of the DCM Dye on the Deduced Room Temperature

Width (cm^{-1})	250	290	310	314	318	325	340	370
Width deviation(%)	21	8.8	2.5	1.3	0	2.2	6.9	16
Temperature deviation(%)	3.3	1.1	0.3	0.1	0	0.2	0.6	1.3

Table VI. Width and Width Fluctuations in Several Dyes Measured with a Quanta-Ray Nd:YAG Dye Laser System

Dye	R 590	R 610	R 640	DCM	Fluore-scein	Kiton Red	Mixture
Width (cm^{-1})	141	130	131	279	144	117	168
Width noise (%)	2.8	3.8	7.6	4.3	1.8	5.3	9.5

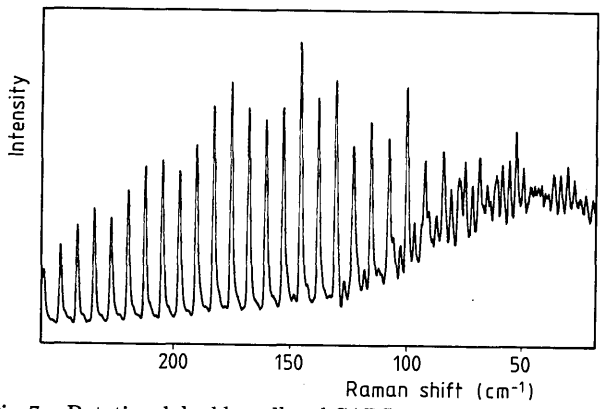

Fig. 7. Rotational dual broadband CARS spectrum from a CO/O_2 diffusion flame indicating peaks from CO ($\gtrsim$100 cm^{-1}) and CO_2 ($\lesssim$100 cm^{-1}).

During the flame experiments the flame was also made fuel rich to investigate the potential for rotational CARS measurements in a sooty environment. It appeared that the rotational CARS spectra were of sufficient quality, even in these conditions, for temperature determinations, although no detailed analyses were made at this point. It might even be an advantage compared to vibrational CARS in which it has been shown that spectral interference from laser-produced C_2 radicals[56] may limit the applicability of this technique, at least in very sooty conditions.[34,57]

Yet another field where rotational CARS might be an alternative to vibrational CARS is in high pressure applications. Since, as mentioned above, the individual rotational transitions are well separated, problems due to pressure effects should not be encountered at moderate pressures. For example, the experimental N_2 CARS spectrum at 38 atm and room temperature, as shown in Fig. 8, has in large been theoretically reproduced without the inclusion of collisional narrowing. Shown in Fig. 8 is also a N_2 CARS spectrum at 1 atm and room temperature for comparison. We intend to carry out detailed investigations in the near future in the areas mentioned above, where the rotational CARS technique seems to have great potential.

VI. Summary and Conclusions

In this paper we report on measurements where single-shot signal intensities and temperature accuracies have been determined for conventional and dual broadband approaches to rotational CARS in flames and room temperature nitrogen. The temperature accuracies are compared to theoretical calculations of the obtainable signal-to-noise (and thereby also the temperature accuracy) of the different techniques as limited by the stochastic nature of the laser radiation. In connection with this, there is a general discussion of how the laser statistics will influence the signal-to-noise ratio. A semiquantitative model for estimating the noise for the dual broadband technique is also described. This is done to provide an intuitive physical picture of how the stochastic properties of laser fields limit the temperature accuracy for these techniques. Experimental results using rotational dual broadband CARS for multiple species detection and in sooty and high pressure environments are discussed as possible situations where rotational CARS may be superior to (or may complement) vibrational CARS. Our computer code for generating theoretical rotational CARS spectra and extracting temperatures from theoretical spectra is also briefly described.

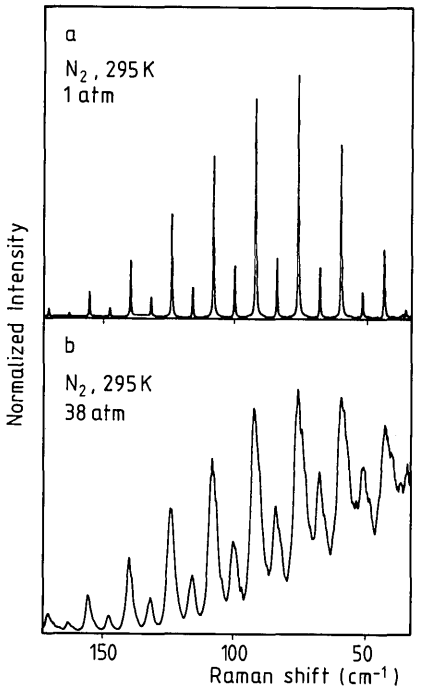

Fig. 8. Rotational dual broadband CARS spectra of room temperature nitrogen: (a) at 1 atm and (b) at 38 atm.

The main general impression from the present work is that if a Nd:YAG laser based system is employed, rotational dual broadband CARS using a single dye surpasses conventional rotational CARS (using a coumarin dye) with regard to signal strength, ease of operation, and temperature accuracy.

Finally, we note that although the work presented in this paper has been directed toward applications of rotational CARS techniques for temperature measurements mainly related to combustion phenomena, the advantages of rotational dual broadband CARS vs conventional rotational CARS are generally valid. Thus the results are relevant for all situations where rotational Raman shifts or small vibrational Raman shifts from heavy molecules are to be studied (e.g., in supersonic expansions) and, dual broadband approaches in general, may be interesting in all experiments where simultaneous recordings of large spectral intervals with good signal-to-noise ratios are required.

We gratefully acknowledge the general interest in this work by S. Svanberg. This work was financially supported by the Swedish Board for Technical Development, STU, and the National Swedish Energy

Board, SEV. This work also forms part of a European collaboration on combustion: the CEC programme Turbulent Combustion & Diagnostics.

References

1. D. R. Crosley, Ed. "Laser Probes for Combustion Chemistry," ACS Symposium Series 134 (American Chemical Society, Washington, DC, 1980).
2. A. C. Eckbreth, *Laser Diagnostics for Combustion Temperature and Species* (Abacus Press, Cambridge, MA, 1987).
3. P. R. Regnier and J. P. E. Taran, "On the Possibility of Measuring Gas Concentrations by Stimulated Anti-Stokes Scattering," Appl. Phys. Lett. **23,** 240–242 (1973).
4. A. C. Eckbreth, "BOXCARS: Crossed-Beam Phase-Matched CARS Generation in Gases," Appl. Phys. Lett. **32,** 421–423 (1978).
5. W. B. Roh, P. W. Schreiber, and J. P. E. Taran, "Single-Pulse Coherent Anti-Stokes Raman Scattering," Appl. Phys. Lett. **29,** 174–176 (1976).
6. D. Klick, K. A. Marko, and L. Rimai, "Broadband Single-Pulse CARS Spectra in a Fired Internal Combustion Engine," Appl. Opt. **20,** 1178–1181 (1981).
7. M. Aldén and S. Wallin, "CARS Experiments in a Full-Scale (10 × 10 m) Industrial Coal Furnace," Appl. Opt. **24,** 3434–3437 (1984).
8. A. C. Eckbreth, "CARS Thermometry in Practical Combustors," Combust. Flame **39,** 133–147 (1980).
9. W. A. England, J. M. Milne, S. N. Jenny, and D. A. Greenhalgh, "Application of CARS to an Operating Chemical Reactor," Appl. Spectrosc. **38,** 867–876 (1984).
10. J. J. Barrett, "Generation of Coherent Anti-Stokes Rotational Raman Radiation in Hydrogen Gas," Appl. Phys. Lett. **29,** 722–724 (1976).
11. I. R. Beattie, T. R. Gilson, and D. A. Greenhalgh, "Low Frequency Anti-Stokes Raman Spectroscopy of Air," Nature London **276,** 378–379 (1978).
12. L. P. Goss, J. W. Fleming, and A. B. Harvey, "Pure Rotational Coherent Anti-Stokes Raman Scattering of Simple Gases," Opt. Lett. **5,** 345-347 (1980).
13. C. M. Roland and W. A. Steele, "Intensities in Pure Rotational CARS of Air," J. Chem. Phys. **73,** 5919–5923 (1980).
14. J. A. Shirley, R. J. Hall, and A. C. Eckbreth, "Folded BOXCARS for Rotational Raman Studies," Opt. Lett. **5,** 380–382 (1980); Y. Prior, "Three-Dimensional Phase Matching in Four-Wave Mixing," Appl. Opt. **19,** 1741–1743 (1980).
15. D. V. Murphy and R. K. Chang, "Single-Pulse Broadband Rotational Coherent Anti-Stokes Raman-Scattering Thermometry of Cold N_2 Gas," Opt. Lett. **6,** 233–235 (1981).
16. J. Zheng, J. B. Snow, D. V. Murphy, A. Leipertz, R. K. Chang and R. L. Farrow, "Experimental Comparison of Broadband Rotational Coherent Anti-Stokes Raman Scattering (CARS) and Broadband Vibrational CARS in a Flame," Opt. Lett. **9,** 341–343 (1984).
17. B. Dick and A. Gierulski, "Multiplex Rotational CARS of N_2, O_2 and CO with Excimer Pumped Dye Lasers: Species Identification and Thermometry in the Intermediate Temperature Range with High Temporal and Spatial Resolution," Appl. Phys. B **40,** 1–7 (1986).
18. A. C. Eckbreth and T. J. Anderson, "Dual Broadband CARS for Simultaneous Multiple Species Measurements," Appl. Opt. **24,** 2731–2736 (1985).
19. A. C. Eckbreth and T. J. Anderson, "Simultaneous Rotational Coherent Anti-Stokes Raman Spectroscopy and Coherent Stokes Raman Spectroscopy with Arbitrary Pump–Stokes Spectral Separation," Opt. Lett. **11,** 496–498 (1986).
20. M. Aldén, P.-E. Bengtsson, and H. Edner, "Rotational CARS Generation Through a Multiple Four-Color Interaction," Appl. Opt. **25,** 4493–4500 (1986).
21. M. Yuratich, "Effects of Laser Linewidth on Coherent Anti-Stokes Raman Spectroscopy," Mol. Phys. **38,** 625–655 (1979).
22. D. R. Snelling, G. J. Smallwood, R. A. Sawchuk, and T. Parameswaran, "Precision of Multiplex CARS Temperatures Using Both Single-Mode and Multimode Pump Lasers," Appl. Opt. **26,** 99–110 (1987).
23. S. Kröll, M. Aldén, T. Berglind, and R. J. Hall, "Noise Characteristics of Single Shot Broadband Raman-Resonant CARS with Single- and Multimode Lasers," Appl Opt. **26,** 1068–1073 (1987).
24. D. R. Snelling, T. Parameswaran, and G. J. Smallwood, "Noise Characteristics of Single-Shot Broadband CARS Signals," Appl. Opt. **26,** 4298–4302 (1987).
25. D. A. Greenhalgh and S. T. Whittley, "Mode Noise in Broadband CARS Spectroscopy," Appl. Opt. **24,** 907–913 (1985).
26. M. Pealat, P. Bouchardy, M. Lefebvre, and J.-P. Taran, "Precision of Multiplex CARS Temperature Measurements," Appl. Opt. **24,** 1012–1022 (1985).
27. A. C. Eckbreth, G. M. Dobbs, J. H. Stufflebeam, and P. A. Tellex, "CARS Temperature and Species Measurements in Augmented Jet Engine Exhausts," Appl. Opt. **23,** 1328–1339 (1984).
28. D. R. Snelling, R. A. Sawchuk, and R. E. Mueller, "Single Pulse CARS Noise: a Comparison Between Single-Mode and Multimode Pump Lasers," Appl. Opt. **24,** 2771–2778 (1985).
29. R. J. Hall and D. A. Greenhalgh, "Noise Properties of Single-Pulse CARS Spectroscopy with Multimode Pump Sources," J. Opt. Soc. Am. B **3,** 1637–1641 (1986).
30. S. Kröll and D. Sandell, "Influence of Laser Mode Statistics on Noise in Nonlinear Optical Processes—Application to Single-Shot Broadband CARS Thermometry," J. Opt. Soc. Am. B **5,** 1910–1926 (1988).
31. S. Kröll, M. Aldén, P.-E. Bengtsson and C. Lüfström, "An Evaluation of Precision and Systematic Errors in Vibrational CARS Thermometry," Appl. Phys. B, in press.
32. R. J. Hall, "CARS Spectra of Combustion Gases," Combust. Flame **35,** 47–60 (1979).
33. R. J. Hall, J. F. Verdieck, and A. C. Eckbreth, "Pressure Induced Narrowing of the CARS Spectrum of N_2," Opt. Commun. **35,** 69–75 (1980).
34. R. J. Hall and L. R. Boedeker, "CARS Thermometry in Fuel-Rich Combustion Zones," Appl. Opt. **23,** 1340–1346 (1984).
35. T. Parameswaran and D. R. Snelling, "A Computer Program to Generate Theoretical Coherent Anti-Stokes Raman Spectra," Defence Research Establishment Ottawa, DREO Technical Note 81-18 (1982).
36. D. Nilsson, "Theoretical and Experimental Investigations of Rotational CARS as a Technique for Temperature Probing," Lund Reports on Atomic Physics, LRAP-76 (1987).
37. G. J. Rosasco and W. S. Hurst, "Measurement of Resonant Third-Order Nonlinear Susceptibilities by Coherent Raman Spectroscopy," Phys. Rev. A **32,** 281–299 (1985).
38. M. C. Drake, "Rotational Raman Intensity-Correction Factors Due to Vibrational Anharmonicity: Their Effect on Temperature Measurements," Opt. Lett. **7,** 440–441 (1982).
39. M. C. Drake, C. Asawaroengchai, and G. M. Rosenblatt, "Temperature from Rotational and Vibrational Raman Scattering: Effects of Vibrational–Rotational Interactions and Other Corrections," ACS Symposium Series 134 (American Chemical Society, Washington, DC, 1980).
40. G. C. Herring, M. J. Dyer, and W. K. Bischel, "Temperature and Density Dependence of the Linewidths and Line Shifts of the Rotational Raman Lines in N_2 and H_2," Phys. Rev. A **34,** 1944–1951 (1986).

41. G. C. Herring, M. J. Dyer, and W. K. Bischel, "Temperature and Wavelength Dependence of the Rotational Raman Gain Coefficient in N_2," Opt. Lett. **11**, 348–350 (1986).
42. F. Y. Yueh and E. J. Beiting, "Analytical Expressions for Coherent Anti-Stokes Raman Spectral (CARS) Profiles," Comput. Phys. Commun. **42**, 65–71 (1986).
43. J. C. Luthe, E. J. Beiting, and F. Y. Yueh, "Algorithms for Calculating Coherent Anti-Stokes Raman Spectra: Application to Several Small Molecules," Comput. Phys. Commun. **42**, 73–92 (1986).
44. H. Kataoka, S. Maeda, and C. Hirose, "Effects of Laser Linewidth on the coherent Anti-Stokes Raman Spectroscopy Spectral Profile," Appl. Spectrosc. **36**, 565–569 (1982).
45. R. E. Teets, "Accurate Convolutions of Coherent Anti-Stokes Raman Spectra," Opt. Lett. **9**, 226–228 (1984).
46. S. Kröll and D. Sandell, "A Model for Calculating the Noise Due to the Stochastic Nature of Multimode Laser Radiation in Nonlinear Optical Processes," in *Proceedings, NLO'88*, organized by the Society for Optical & Quantum Electronics (1988).
47. A. C. Eckbreth, T. J. Anderson, and G. M. Dobbs, "Multi-Color CARS for Hydrogen-Fueled Scramjet Applications," Appl. Phys. B **45**, 215–223 (1988).
48. R. L. Farrow, R. P. Lucht, and L. A. Rahn, "Measurements of the Nonresonant Third-Order Susceptibilities of Gases Using Coherent Anti-Stokes Raman Spectroscopy," J. Opt. Soc. Am. B **4**, 1241–1246 (1987).
49. T. Lasser, E. Magens, and A. Leipertz, "Gas Thermometry by Fourier Analysis of Rotational Coherent Anti-Stokes Raman Scattering," Opt. Lett. **10**, 535–537 (1985).
50. A. Leipertz, E. Magens, and T. Lasser. "Flame Temperature Measurements Using a Novel Rotational CARS Analysis Technique," presented at AIAA Eighteenth Fluid Dynamics and Plasma Dynamics and Laser Conference, Cincinnati, OH (16–18 July 1985).
51. A. V. Masalov, "Spectral and Temporal Fluctuations of Broadband Laser Radiation," Prog. Opt. **22**, 145–196 (1985).
52. Z. W. Li, C. Radzewicz, and M. G. Raymer, "Temporal Smoothing of Multimode Dye-Laser Pulses," Opt. Lett. **12**, 416–418 (1987).
53. C. Radzewics, Z. W. Li, and M. G. Raymer, "Amplitude-Stabilized Chaotic Light," Phys. Rev. A **37**, 2039–2047 (1988).
54. D. R. Snelling, G. J. Smallwood and R. A. Sawchuck, "Nonlinearity and Image Persistence of P-20-Phosphor-Based Intensified Photodiode Array Detectors used in CARS Spectroscopy," Appl. Opt. in press.
55. C. M. Penney, R. L. St. Peters, and M. Lapp, "Absolute Rotational Raman Cross Section for N_2, O_2, and CO_2," J. Opt. Soc. Am. **64**, 712–716 (1974).
56. A. C. Eckbreth and R. J. Hall, "CARS Thermometry in a Sooting Flame," Combust. Flame **36**, 87–98 (1979).
57. P.-E. Bengtsson, D. Nilsson, M. Aldén and S. Kröll, "Vibrational CARS Thermometry in Sooty Flames," to be published.

Of Optics *continued from page 3043*

density, he said. In wires, "as you increase the speed, the internal resistance increases," and, given the proximity of the multiple connections, "they begin talking to each other, acting as antennas." Fiber optic links have no resistance, and because light is different from electricity, many different signals can be sent simultaneously over a single cable.

Other researchers in the field say that the Sarnoff chip is an important development, but add that it is only one way to address the problem. Some scientists are developing optoelectronic chips with fewer lasers but more electronic components, which they say have more potential for near term development. Others are looking at more esoteric materials and fabrication technologies to pack still more lasers into less space. The International Business Machines Corp. has developed chips of gallium arsenide with up to 10,000 transistors and four optical devices. "We felt that what was important was not just combining one or two transistors and an optical device; it was important to be able to put thousands of electronic devices together with a few optical devices," said John Crow, manager of an optical technology group at IBM Research. "That makes it possible on a single chip to handle not only the light process but the data handling as well," he said. "It's a much more useful chip."

At the American Telephone & Telegraph Co., researchers have taken a different approach, attempting to integrate a number of different types of optical device on a single chip. The company recently showed what is known as a photonic integrated circuit. It combines three lasers whose light can be adjusted to different colors, or frequencies, and sent over a single fiber optic cable. One use of such devices would be to increase the number of signals that could be sent on one fiber optic cable—from 25,000 today to as many as a billion, said Thomas L. Koch, a supervisor in the photonics circuits department at AT&T's Bell Laboratories. He said he expected optical data transmission to find a substantial market beyond telecommunications alone. "In order to break into this area and make it even remotely practical you need much more complex photonic devices," Koch said. "We are not trying to make the systems of today in a more economical way; we are trying to make systems that don't exist today."

Both the AT&T and IBM devices are built in gallium arsenide, which while relatively new, is a commercially available material. The Sarnoff researchers concede that their sandwich of gallium arsenide and silicon is still too defect-prone for mass production, but believe they can overcome that problem. Researchers at universities in the United States and abroad are working with still more exotic materials, seeking to put even more devices in less space. The Sarnoff chip "is a very nice structure, very practical," said Larry A. Coldren, a professor of materials and electrical and computer engineering at the University of California at Santa Barbara. "We have a pretty good alternative, though it is further out in terms of practicality." Unlike the Sarnoff chip, in which light moves parallel to its surface until it strikes the grate and reflects out, the Santa Barbara device propagates light perpendicular to the surface in minute cavities between its different layers of semiconductor material. "The advantage of the structure is that it is much smaller," Coldren said. "In building integrated circuits, the name of the game is to squeeze as many devices in as small a space as you can." This permits greater complexity, higher speed and ultimately lower cost. The drawback to this design is it does not dissipate heat as well as the Sarnoff chip.

Scientists are confident that they can move beyond problems of heat and inconsistent materials. Optoelectronics will also require radical changes in basic computer design. "This is a high risk for any individual company," Ettenberg said. "I think there will have to be a joint venture, at least to start the product out and get something going." He said a government-backed consortium of companies, like Sematech, was essential to compete with large scale efforts by the Japanese.